SIMULATION OF AN ISOLATED WIND HYDRO SYSTEM

R. Sebastián[(a)], J. Quesada[(b)]

[(a)] Department of Electrical, Electronic and Control Engineering (DIEEC), Spanish University for Distance Education, UNED 28040 Madrid, Spain
[(b)]University of the Basque Country UPV/EHU, E.U.I. Vitoria-Gasteiz, Nieves Cano 12, 01006 Vitoria-Gasteiz, Spain

[(a)]rsebastian@ieec.uned.es, [(b)]jeronimo.quesada@ehu.es

ABSTRACT
In this paper it is presented the modeling and the dynamic simulation of a Wind Hydro isolated Power System (WHPS) consisting of a Hydraulic Turbine Generator (HTG), a Wind Turbine Generator (WTG), the consumer Load and a Dump Load. The models of the hydraulic turbine along with its penstock and the wind turbine are presented. The Synchronous Machine of the HTG provides the isolated system voltage waveforms so the HTG must be always running. The used hydraulic turbine speed governor is isochronous so that the isolated system frequency will be kept in its rated value. The WTG provides active power to the isolated system when enough wind is available and its induction generator consumes reactive power. The WHPS is simulated for a positive load step and a positive wind speed step and graphs for the main system variables: system frequency and voltage and active powers of each component of the WHPS are presented. The simulations show how the WTG induction generator increases the system stability.

Keywords: Wind Turbine Generator, Hydro Turbine Generator, Isolated microgrid, Power systems Simulation

1. INTRODUCTION

Remote microgrids (RMG) are microgrids [Lasseter 2002] and [Basak et al. 2012] deployed in remote geographical areas either isolated from the distribution grid or with an intermittent or low-reliability connection to it. Isolated power systems are traditionally based on diesel generators (DG) but when combined with renewable energy sources and energy storage [Sebastian 2013], they acquire the characteristics of a microgrid. Wind power and Hydro power are two sources of renewable energy. Both types of renewable energy are site dependent, enough available wind is needed for wind power and a river and the possibility of building a dam is needed for hydro power. Fig.1 shows a Hydraulic turbine (HT) driving a Synchronous Machine (SM) forming a Hydraulic Turbine generator (HTG) and a Wind Turbine driving an Induction Generator (IG) forming a Wind Turbine Generator (WTG). Both HTG and WTG are combined to form an isolated Wind Hydro Power System (WHPS) to supply the isolated community electric load. Also a DL is in Fig.1 to balance active power when an excess of generating power exists.

In the WHPS of Fig. 1 the HTG is always running since the SM generates the voltage waveform of the isolated grid. The WTG will be connected to the isolated grid when enough wind is available. Two operation modes are possible in the WHPS of Fig.1: Hydro Only (HO) mode where the HTG supplies all the demanded active and reactive power (WTG is disconnected) and Wind Hydro (WH) mode where in addition to HTG the WTG also supply active power.

2. THE ISOLATED POWER SYSTEM

The hydraulic turbine (HT) converts water pressure into mechanical shaft power (Paish 2002). As Fig. 1 shows the HT drives the Synchronous generator SM. The hydraulic turbine is modeled with a nonlinear turbine model. Non-linear turbine models are required when speed and power changes are large during the hydraulic turbine operation which is the case of this article. The mechanical power produced by the HT $P_{h\text{-}mec}$ is proportional to the product of the effective pressure head of water above the turbine H, the volume flow rate passing through the turbine Q and the hydraulic efficiency of the turbine η:

$$P_{h\text{-}mec} = \rho g H Q \eta \quad (1)$$

where ρ is the density of water and g is the acceleration due to gravity. Another way to take into account the hydraulic efficiency η if it is assumed constant and independent of Q, is to consider in eq. (1) an effective flow which is the difference of actual flow Q from the no load flow Q_{nl}:

$$P_{h\text{-}mec} = (Q - Q_{nl})\rho g H \quad (2)$$

The mechanical power produced by a HT is varied to meet variations in load demand by regulating the turbine flow rate Q. For this aim a needle valve is used in impulse type turbines and a wicket gate is used in

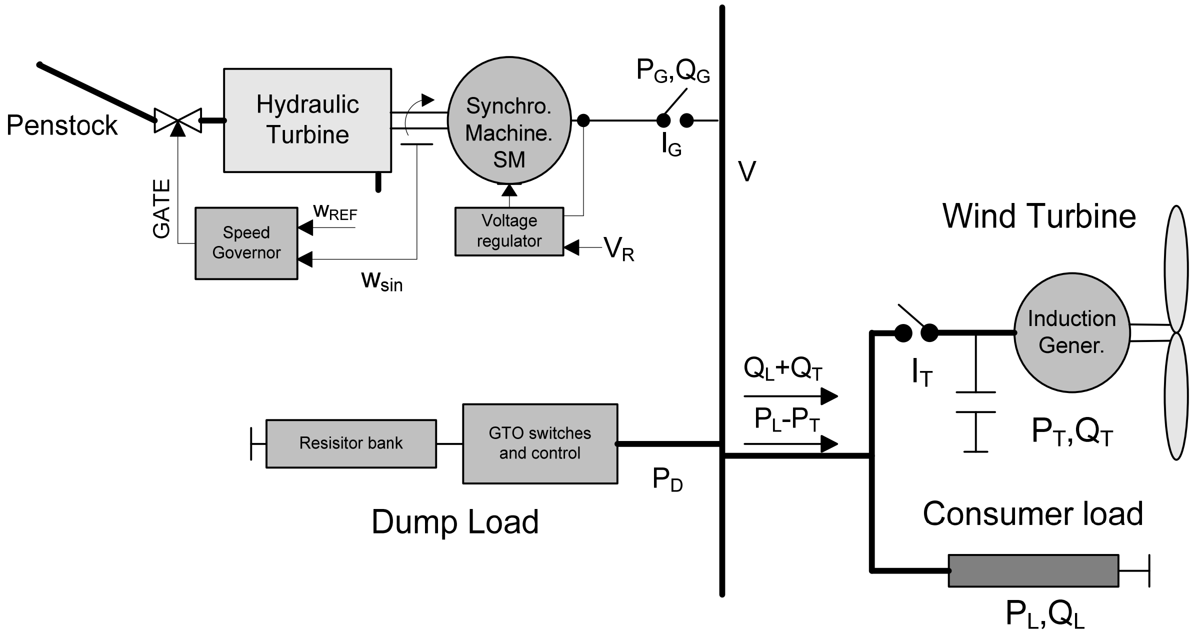

Fig. 1. Layout of the Wind-Hydro isolated Power System

reaction type turbines (Lucero 2010). The pressure head above the turbine per unit h is related to the per unit flow rate q by assuming that the turbine can be represented by the valve characteristic:

$q = yh^{1/2}$ (3)

where y is the turbine gate opening position, which has values from 0 (fully closed) to 1 fully open, $q= Q/Q_{base}$, where Q_{base} is the turbine flow rate with the gate fully open and $h=H/H_{base}$, where H_{base} is the total available static head above the turbine (Mello et al. 1992).

Equation (2) in per unit power on SM rated power base and taking into account a speed deviation effect which is a function of the gate opening y can be expressed as (Mello et al. 1992):

$p_{h\text{-}mec} = A_t(q - q_{nl})h - K_D y(\omega\text{-}1)$ (4)

where q_{nl} is the no load flow rate per unit, $(\omega\text{-}1)$ is the difference between the actual HT speed in per unit ω and the rated turbine speed 1 pu, K_D is the damping torque coefficient and A_t is a proportionality factor and is assumed constant. A_t is calculated using HT active rated power and SM apparent rated power (Mello et al. 1992).

The penstock is a pressure pipe that conveys the water to the turbine. The penstock is modeled assuming an inelastic conduit and incompressible fluid. Also the traveling pressure wave effects are neglected, so that this penstock model is valid only for short-medium lengths penstocks. If the penstock has length L (m), an area A (m^2), H_o and H are the static heads of water column at the beginning and end of the penstock respectively and the H_f is head loss due to friction in the penstock, the second Newton´s law applied to the penstock gives (Mello et al. 1992):

$$\frac{dQ}{dt} = \frac{gA}{L}(H_o - H - H_f) \quad (5)$$

Eq. (5) expressed in per unit values becomes:

$$\frac{dq}{dt} = \frac{1}{T_W}(1 - h - h_f) \quad (6)$$

where T_W is the water time constant or water starting time (secs) defined as:

$$T_W = \frac{L}{Ag}\frac{Q_{base}}{H_{base}} \quad (7)$$

In the simulations ahead the penstock friction losses H_f in eq. (5) and the damping torque coefficient K_D in eq. (4) are considered null, so that the system stability of the WHPS simulated will be worse since these natural damping are not taking into account.

The SM of Fig. 1 generates the voltage waveform of the isolated grid and its automatic voltage regulator controls the system voltage to be within the prescribed levels. For this reason the SM must be always running close to its rated speed. The SM has a rated power ($P_{SM\text{-}NOM}$) of 300 kVA, it receives the HT mechanical output power and converts it in electrical power. The SM electrical part is represented by a sixth-order model. An IEEE type 1 Voltage regulator plus an exciter regulates the voltage in the SM terminals.

The WTG in Fig.1 consists of a Wind Turbine (WT) driving an Induction Generator (IG) directly connected to the autonomous grid conforming a constant speed stall-controlled WTG (no pitch control).

The mechanical power produced by a WT (Sebastian and Peña 2011) is:

$$P_{T-MEC} = \frac{1}{2}\rho A v^3 C_P \quad (8)$$

where ρ is the air density, v is the wind speed, A is the area swept by the turbine blades and C_P is the power coefficient. C_P is a function of the Tip Speed Ratio (TSR=$R\omega_r/v$, where R is the blade length and ω_r is the WT shaft speed) and the blade pitch. Since the WTG used in this paper has no pitch control, C_P is only a function of TSR. In addition, the IG speed range variation in the WTG is very limited and thus C_P can be considered in first approximation as a function only of the wind speed. As the wind speed is quasi-random there is no way to control the active power that the WTG produces, so the WTG behaves as an uncontrolled source of active power. The IG consumes reactive power so a capacitor bank has been added in Fig. 1 to compensate the power factor. The simulated constant speed stall controlled WTG model follows the one in (Gagnon et al. 2002) and has an Induction Generator (IG) of 275 kW (WTG rated power $P_{T\text{-}NOM}$ = 275 kW) and the Wind Turbine (WT) block described later. The electrical part of the IG is represented by a fourth-order model. Typical inertia constant H_W values for WTGs are between 2 and 6 seconds (Knudsen and Nielsen 2005). As the WTG used in the article is a low power one, the low limit of the previous range, 2 seconds, is assigned to H_W.

The Dump Load (DL) of Fig.1 consists of a set of semiconductor power switches and a bank of resistors. By closing/opening these power switches, the DL consumed active power can be controlled behaving as a controlled sink of active power. The DL of (Sebastián and Peña 2010) is used and consists of eight three phase resistors connected in series with GTO switches. The resistors values follow an 8 bit binary progression so that the power consumed by the DL, assuming that the voltage in the isolated grid is nominal, can be expressed in the form:

$$(I_0+I_1\cdot 2^1+..+I_7\cdot 2^7)\cdot P_{STEP} = X_{D\text{-}REF}\cdot P_{STEP} \quad (9)$$

(9) means that the power can be varied discretely from 0 to 255·P_{STEP}, where P_{STEP} is the power corresponding to the least significant bit and I_J is "1" when the associated GTO is turned on and "0" when the GTO is turned off. For this article P_{STEP} = 1.4 kW and therefore $P_{D\text{-}NOM}$ = 357 kW. The DL is used in the isolated WHPS to consume power when there is an excess of generated power. This active power consumption is temporary until the HTG has adjusted its produced power to the needed power. In other isolated hydro power systems (Paish 2002) the HTG always run at full power and speed control is achieved by adjusting the DL consumed power instantly so that the sum of the powers consumed by the load and the DL is equal to the HTG generated power.

2.1. The HT speed governor system

The isolated power system frequency f is regulated by maintaining an instantaneous balance of the active power consumed and produced. The HT/SM shaft speed ω (rad/s) is related with the system frequency (frequency of the voltage waveform) f (Hz) by:

$$\omega = 2\pi f/p \quad (10)$$

with p the number of pole pairs of the SM. The used SM in this article has p=16 and the isolated system frequency is f= 60 Hz, so the HTG rated speed is 187.5 rpm.

The HT speed governor modulates the HT produced power in order to accomplish active power balance, so the HT behaves as a controlled source of active power. To vary HT produced power, the HT governor regulates the inlet of water into the turbine through the gate variable as explained previously.

The speed control of the HT used in this article is isochronous, so the HT will run at constant speed provided that the HT demanded load is in the range spanning from 0 to its rated power. The HT governor consists of a PID speed regulator and a servo which converts the speed regulator output in the corresponding GATE opening. As the speed control is isochronous, the speed controller does not include permanent speed droop, which can help to improve the power system stability in isolated operation. The PID K_p, K_i and K_d parameters are calculated according to (Hagihara et al. 1979):

$$K_p = 1.6H/T_W \quad (11)$$

$$K_i = 0.48Kp/(3.33T_W) \quad (12)$$

$$K_d = 0.54H \quad (13)$$

where H is the HTG inertia constant (secs) and T_W is the previously defined water time constant. For a low speed HTG (< 200 rpm) as the present case H is between 2-3 seconds (Kothariand and Nagrath 2003). The first figure of the previous range is applied to H, as the HTG used in the article is a low power one. For the penstock it is assumed a short length one with T_W= 1 sec. With H=2 secs for the HTG and T_W= 1 sec for the penstock, the parameters in (11)-(13) are calculated conforming the PID speed controller used in the described simulations below.

3. SIMULATION RESULTS

The isolated WHPS of Fig.1 were simulated using the MATLAB-Simulink multipurpose simulation software [Matlab 2014]. The WHPS Simulink schematic can be seen in Fig. 2. Some of the components described previously and shown in Fig.2, such as the IG, the SM and its voltage regulator, the consumer load, etc. are blocks which belong to the SimPowerSystems library for Simulink. The Hydro Turbine block implements all the equations (1) to (7) that described the HT, gate and penstock behavior. It receives as inputs the constant 1 pu speed reference, the current HTG speed ω and deviation speed $d\omega$ and outputs the mechanical power $P_{h\text{-}mec}$ to take the HTG speed to 1 pu speed reference.

The WT block of Fig. 2 contains the wind turbine power curves which define the mechanical power in the WT shaft $P_{T\text{-}MEC}$ as a function of the wind speed and the WT shaft speed as it is described in eq. (8). This $P_{T\text{-}MEC}$ is divided by the WT speed to calculate the mechanical torque applied to the WTG-IG.

For sake of clarity the DL is not shown in Fig.2 as the DL is not needed throughout the tests presented ahead (the HTG accommodates it output power to the consumer load and WTG power variations) so the DL does not actuate and its consumed active power is zero.

The results of the simulation are shown with the following variables: the frequency per unit (fpu) and WTG-IG speed per unit (Fig 3), the RMS voltage per unit (Fig 4) and the active powers for the WTG, HTG, and consumer load (Fig 5) in kW. In Fig. 5 the active power is considered positive if produced and negative if consumed. At the test starting point the wind speed is 7 m/s, the WTG and HTG are producing active powers of 50 kW and 200 kW respectively and the load is consuming active power of 250 kW being the system at steady state.

In t=1 s the extra 30 kW resistive load is connected to the system (10% of the HTG rated power) by closing the 3 phase breaker of Fig. 2 as it can be observed in the load active power curve in Fig. 5. Fig. 5 also shows that the load power oscillates due to the voltage variations (minimum-maximum: 0.9806-1.0074 pu) observed in Fig. 4 after the connection of this extra load (main and extra loads are purely resistive). Additionally Fig. 5 shows that the wind power presents a transient due to the 30 KW positive load step. Fig. 3 shows that the system frequency reduction after the load step contributes to increase sharply the difference between the WTG-IG speed and the fpu (IG slip). The WTG active power is approximately proportional to the IG slip, so the IG slip increase makes the WTG to instantaneously increase power production at expense of its kinetic energy as Fig 5 shows. This is a desirable effect since counter acts the frequency dip by providing more power to the grid, increasing the damping and therefore the isolated power system stability. In steady state the wind power has the same value as the initial one in t=0, since the wind speed has not changed. Fig. 3 shows that the IG speed is greater than the fpu (IG slip positive) during the load step transient so that the WTG behaves as a generator the whole transient. The fpu/IG speed minimums and maximums are 0.9743 (-2.57%)/0.9772 and 1.0043/1.0072, and both responses are lightly over oscillating. Fig. 5 shows that the power in the HTG increases with oscillations at the beginning of the load step and at steady state reached at t= 28,268 s, the HTG assumes the increase of load with a final power of 230 kW.

In Fig. 3 it is also plotted the system fpu response to the +30 kW extra load in HO mode, i.e. with only the HTG supplying the consumer load (WTG disconnected). It can be seen that the fpu minimum and maximum are 0.9529 (-4.71%) and 1.0145 respectively and the fpu response is over oscillating. If the HO fpu response it is compared with the previous fpu in WH mode, it is demonstrated that when the WTG also supplies power, the WTG adds damping so that the isolated power system stability is greater.

In t = 41 s the wind speed changes suddenly from its initial value of 7 m/s to 8 m/s. Fig 3 shows that the IG slip increases, but its variation is smoother than in the load step case since in this case the system frequency increases and part of the captured wind power is converted in WTG kinetic energy. Fig. 5 shows the corresponding increasing in the WTG power

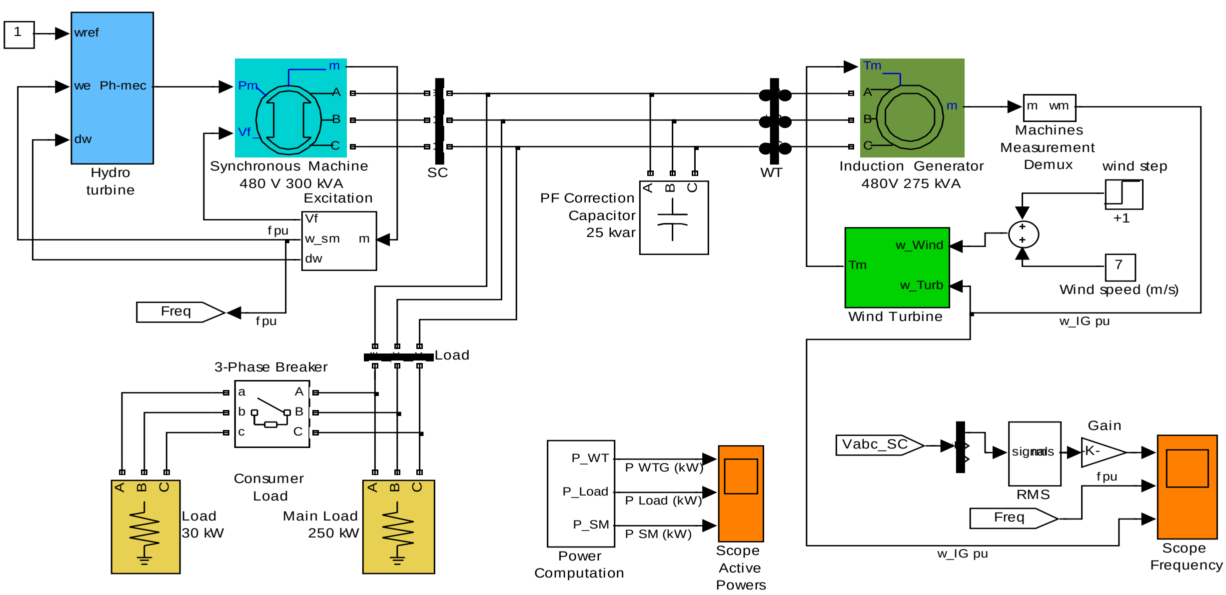

Fig. 2. Wind-Hydro isolated Power System Simulink schematics

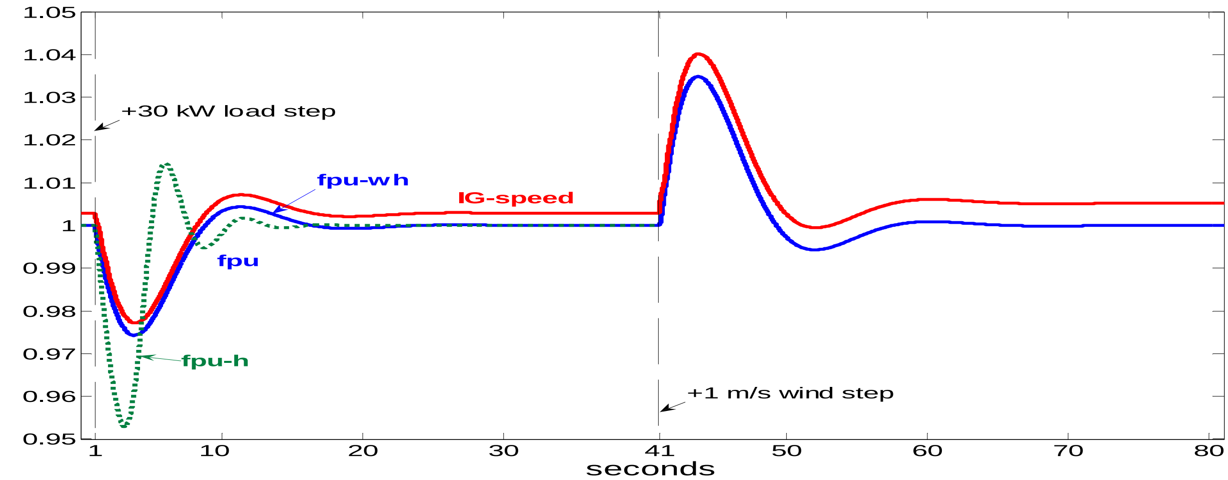

Fig. 3. Frequency and IG generator speed per unit

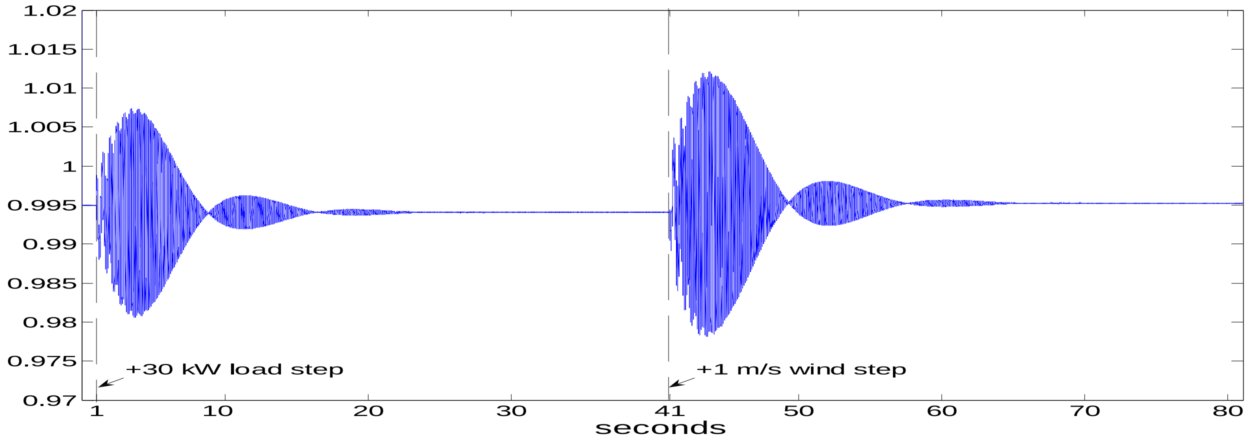

Fig. 4. RMS Voltage per unit

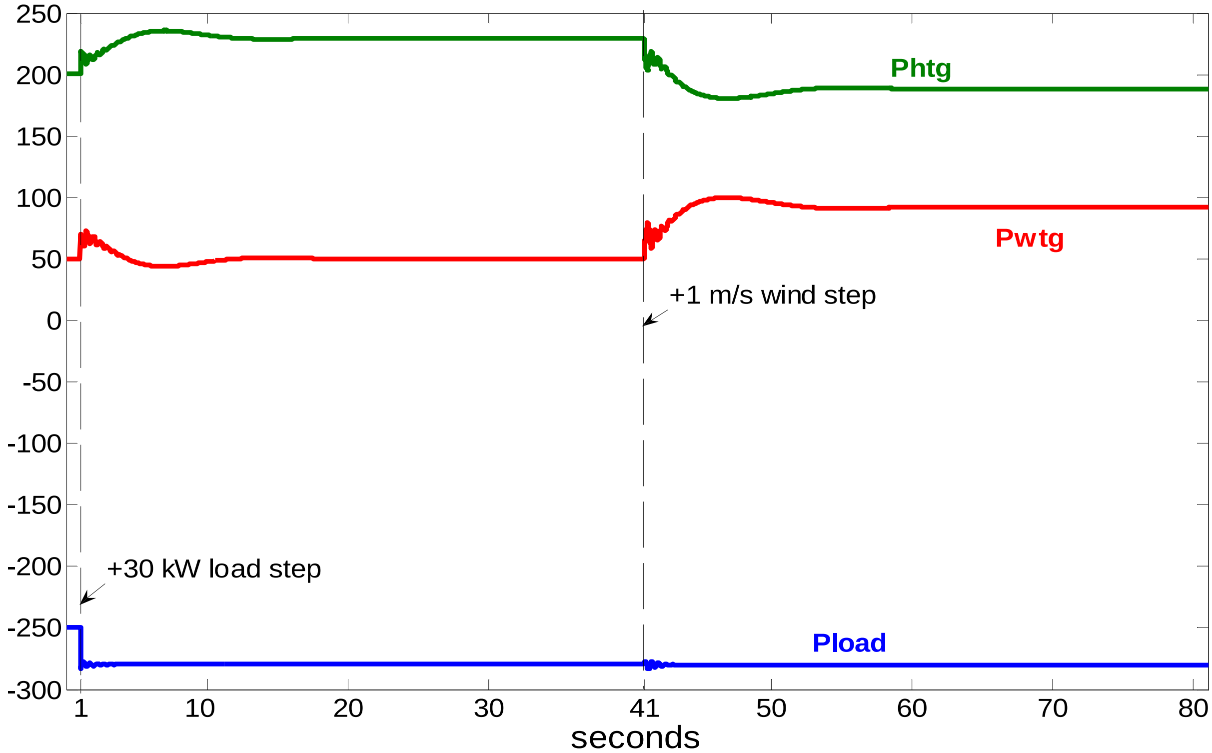

Fig. 5. Generated(+)/consumed(-) active Powers (kW) by the WTG, HTG and Load

from its initial 50 kW value to 92 KW in steady state. Fig. 3 shows fpu/IG speed maximums of 1.0348 (+3.48%)/1.0402 being in addition both responses under oscillating. The minimum–maximum voltages during this wind step are 0.9781-1.0121pu. Fig. 5 shows that the HTG active power decreases with oscillations at the beginning of the wind step. In steady state, reached at t = 59.188 s the HTG accommodates its output power to the new situation generating 188 kW.

4. CONCLUSSIONS

The WDPS model has been presented and tested for positive load and wind steps. The detailed models of the HT and its penstock and the WT have been described. The simulations show the damping that the WTG adds to the isolated system increasing the power system stability.

ACKNOWLEDGMENTS

The authors would like to thank the DIEEC-UNED for supporting partly the attendance to the conference.

REFERENCES

Basak P., S. Chowdhury, S. Halder nee Dey, S.P. Chowdhury, A literature review on integration of distributed energy resources in the perspective of control, protection and stability of microgrid, Renew. Sustain. Energy Rev. 16 (2012) 5545–5556.

Gagnon, R.; Saulnier, B.; Sybille, G.; Giroux, P.: “Modelling of a Generic High-Penetration No-Storage Wind-Diesel System Using Matlab/Power System Blockset”, 2002 Global Windpower Conference, April 2002, Paris, France

Hagihara, S. et al, 1979, Stability of a Hydraulic Turbine Generating Unit Controlled by P.I.D. Governor, Power Apparatus and Systems, IEEE Transactions on, 1979.PAS‐98(6): p.2294‐2298.

Knudsen H., Nielsen J. N., Introduction to the modeling of wind turbines, In *Wind Power in Power Systems*, T. Ackermann, Ed. Chicester, U.K. Wiley, 2005, pp. 525–585

Kothari, D. P. , Nagrath I. J., Modern power system analysis, Tata McGraw-Hill Education, 2003

Lasseter R., Microgrids, in: Proceedings of the IEEE PES Winter Meeting, vol. 1, 2002, pp. 305–308.

Lucero L.A., 2010. Hydro Turbine and Governor Modelling: Electric - Hydraulic Interaction, Master Thesis, June 2010, Norwegian University of Science and Technology

Matlab 2014, The MathWorks Inc., “Matlab –Simulink documentation”, available in: http://www.mathworks.es/es/help/index.html

Mello F.P. et al, Hydraulic turbine and turbine control models for system dynamic studies. Power Systems, IEEE Transactions on, 1992. 7(1): p. 167‐179.

Paish O., 2002. Small hydro power: technology and current status, Renewable and Sustainable Energy Reviews, Volume 6, Issue 6, December 2002, Pages 537-556, ISSN 1364-0321, http://dx.doi.org/10.1016/S1364-0321(02)00006-0.

Sebastián R., Peña Alzola R., 2010 , Effective active power control of a high penetration wind diesel system with a Ni–Cd battery energy storage, Renewable Energy, Volume 35, Issue 5, May 2010, Pages 952-965, ISSN 0960-1481, http://dx.doi.org/10.1016/j.renene.2009.11.029.

Sebastian R., 2011, Modelling and simulation of a high penetration wind diesel system with battery energy storage, International Journal of Electrical Power & Energy Systems, Volume 33, Issue 3, March 2011, Pages 767-774, ISSN 0142-0615, http://dx.doi.org/10.1016/j.ijepes.2010.12.034.

Sebastián R., Peña Alzola R., 2011. Simulation of an isolated Wind Diesel System with battery energy storage, Electric Power Systems Research, Volume 81, Issue 2, February 2011, Pages 677-686, ISSN 0378-7796, http://dx.doi.org/10.1016/j.epsr.2010.10.033.

Sebastián R., 2013. Reverse power management in a wind diesel system with a battery energy storage, International Journal of Electrical Power & Energy Systems, Volume 44, Issue 1, January 2013, Pages 160-167, ISSN 0142-0615, http://dx.doi.org/10.1016/j.ijepes.2012.07.029.